Available online at www.sciencedirect.com
SCIENCE DIRECT®
International Journal of Heat and Fluid Flow 25 (2004) 1047–1051
International Journal of HEAT AND FLUID FLOW
www.elsevier.com/locate/ijhff

A robust near-wall elliptic-relaxation eddy-viscosity turbulence model for CFD

K. Hanjalić, M. Popovac *, M. Hadžiabdić

Department of Multi-Scale Physics, Faculty of Applied Sciences, Delft University of Technology, Lorentzweg 1, 2628 CJ Delft, Netherlands

Received 20 April 2004; received in revised form 6 July 2004; accepted 15 July 2004

Abstract

An eddy-viscosity model based on Durbin's elliptic relaxation concept is proposed, which solves a transport equation for the velocity scales ratio $\zeta = \overline{v^2}/k$ instead of $\overline{v^2}$, thus making the model more robust and less sensitive to grid nonuniformities. Computations of flows and heat transfer in a plane channel, behind a step and in a round impinging jet show all satisfactory results.

Keywords: CFD; RANS; Elliptic relaxation; ζ–f model

1. Introduction

The $\overline{v^2}$–f model of Durbin (1991) appeared as an interesting novelty in engineering turbulence modelling. By introducing an additional ("wall-normal") velocity scale $\overline{v^2}$ and an elliptic relaxation concept to sensitize $\overline{v^2}$ to the inviscid wall blocking effect, the model dispenses with the conventional practice of introducing empirical damping functions. Because of its physical rationale and of its simplicity, it is gaining in popularity and appeal especially among industrial users. Whilst in complex three-dimensional flows, with strong secondary circulation, rotation and swirl, where the evolution of the complete stress field may be essential for proper reproduction of flow features the model remains still inferior to second-moment and advanced non-linear eddy viscosity models, it is certainly a much better option than the conventional near-wall k–ε and similar models.

However, the original $\overline{v^2}$–f model possesses some features that impair its computational efficiencies. The main problem is with the wall boundary condition for f, i.e. $f_w = \lim_{y\to 0} - 20\overline{v^2}\nu^2/(\varepsilon y^4)$, which makes the computations sensitive to the near-wall grid clustering and—contrary to most other near-wall models—does not tolerate too small y^+ for the first near-wall grid point. The problem can be obviated by solving simultaneously the $\overline{v^2}$ and f equations, but most commercial as well as in-house codes use more convenient segregated solvers. Alternative formulations of the $\overline{v^2}$ and f equations have been proposed which permit $f_w = 0$ (Lien et al., 1998), but these perform less satisfactory than the original model and require some re-tuning of the coefficients.

We propose a version of eddy-viscosity model based on Durbin's elliptic relaxation concept, which solves a transport equation for the velocity scales ratio $\zeta = \overline{v^2}/k$ instead of the equation for $\overline{v^2}$. The motivation behind this development originated from the desire to improve the numerical stability of the model, especially when using segregated solvers. Because of a more convenient formulation of the equation for ζ and especially of the wall boundary condition for the elliptic function f, it is more robust and less sensitive to nonuniformities and clustering of the computational grid. Another novelty is the application of a quasi-linear pressure–strain model in the f-equation, based on the formulation of Speziale et al. (1991) (SSG), which brings additional

* Corresponding author.
E-mail address: mirza@ws.tn.tudelft.nl (M. Popovac).

0142-727X/$ - see front matter
doi:10.1016/j.ijheatfluidflow.2004.07.005

improvements for non-equilibrium wall flows. The computations of flow and heat transfer in a plane channel, behind a backward facing step and in a round impinging jet show in all cases satisfactory agreement with experiments and direct numerical simulations. [1]

2. The ζ–f model

The ζ equation can be derived directly from the $\overline{\upsilon^2}$ and k equations of Durbin (1991). The direct transformation yields:

$$\frac{D\zeta}{Dt} = f - \frac{\zeta}{k}\mathscr{P} + \frac{\partial}{\partial x_k}\left[\left(\nu + \frac{\nu_t}{\sigma_\zeta}\right)\frac{\partial \zeta}{\partial x_k}\right] + X \quad (1)$$

where the "cross diffusion" X is a consequence of transformation and can be written in a condensed form as:

$$X = \frac{2}{k}\left(\nu + \frac{\nu_t}{\sigma_\zeta}\right)\frac{\partial \zeta}{\partial x_k}\frac{\partial k}{\partial x_k} \quad (2)$$

The solution of the ζ equation (1) instead of $\overline{\upsilon^2}$ should produce the same results. However, from the computational point of view, two advantages can be identified:

- instead of ε appearing in the $\overline{\upsilon^2}$ equation, which is difficult to reproduce correctly in the near-wall layer, the ζ equation contains the turbulence kinetic energy production $\mathscr{P}$ which is much easier to reproduce accurately if the local turbulent stress and the mean velocity gradient are captured properly—what is the main goal of all models.
- because $\zeta \propto y^2$ when $y \to 0$, the wall boundary condition for ζ deduced from the budged of ζ equation in the limit when the wall is approached reduces to the balance of only two terms (with X neglected, see below) with a finite value at the wall, elliptic relaxation function f and the viscous diffusion $\mathscr{D}^\nu\zeta$, whereas $\mathscr{P}\zeta/k$ varying with y^3 (in fact with y^4 when eddy viscosity is used) goes to zero at the wall:

$$f_{\mathrm{w}} = \lim_{y\to 0}\frac{-2\nu\zeta}{y^2} \quad (3)$$

This is a more convenient and easier reproducible form as compared with f_w in the $\overline{\upsilon^2}$–f model. In fact, the boundary condition for f_w has the identical form as that for ε_w and can be treated jointly in the computational procedure.

The mere fact that both the nominator and the denominator of f_w are proportional to y^2 instead of y^4 as in the original $\overline{\upsilon^2}$–f model (with $y = 0$ being a singular point in both cases), brings improved stability of the computational scheme. However, in order to reduce the ζ equation to a simple source-sink-diffusion form, we can omit the term X. This term is not significant, though close to the wall it has some influence. In order to compensate for the omission of X one can re-tune some of the coefficients. Furthermore some additional improvements can be introduced as follows below.

3. The ζ–f model with quasi-linear pressure–strain term

Instead of using the simple linear IP model for the rapid part of the pressure–strain term as practiced in the conventional $\overline{\upsilon^2}$–f model, we can adopt the more advanced quasi-linear model of Speziale et al. (1991):

$$\Pi_{ij,2} = -C_2'\mathscr{P}a_{ij} + C_3kS_{ij} + C_4k\left(a_{ik}S_{jk} + a_{jk}S_{ik} - \frac{2}{3}\delta_{ij}a_{kl}S_{kl}\right) + C_5k(a_{ik}\Omega_{jk} + a_{jk}\Omega_{ik}) \quad (4)$$

which was found to capture better the stress anisotropy in wall boundary layers. Application to the wall normal stress component, with $\mathscr{P}_{22} = 0$ yields the following form of the f equation in conjunction with the ζ equation (1) (with $X = 0$):

$$L^2\nabla^2 f - f = \frac{1}{\tau}\left(c_1 + C_2'\frac{\mathscr{P}}{\varepsilon}\right)\left(\zeta - \frac{2}{3}\right) - \left(\frac{C_4}{3} - C_5\right)\frac{\mathscr{P}}{k} \quad (5)$$

where L and τ are length and time scale, respectively, and $c_1 = C_1 - 1 = 0.4$ is introduced for simplicity. We adopted the coefficients for the SSG pressure–strain model, but with $C_2' = 0.65$: (its original SSG value 0.9 was reduced by about 25% on the same ground as Durbin reduced in similar proportion the original value of C_1 in order to take into account the discrepancy in the definition of ε in the log-law region) Noting that the last term in Eq. (5) can be neglected as compared with the first term because $(C_4/3 - C_5) \approx 0.008$, we arrive to the following set of model equations constituting the ζ–f (with $C_\mu = 0.22$ as in the $\overline{\upsilon^2}$–f model of Durbin):

$$\nu_t = C_\mu \zeta k \tau \quad (6)$$

$$\frac{Dk}{Dt} = \mathscr{P} - \varepsilon + \frac{\partial}{\partial x_j}\left[\left(\nu + \frac{\nu_t}{\sigma_k}\right)\frac{\partial k}{\partial x_j}\right] \quad (7)$$

$$\frac{D\varepsilon}{Dt} = \frac{(C_{\varepsilon 1}\mathscr{P} - C_{\varepsilon 2}\varepsilon)}{\tau} + \frac{\partial}{\partial x_j}\left[\left(\nu + \frac{\nu_t}{\sigma_\varepsilon}\right)\frac{\partial \varepsilon}{\partial x_j}\right] \quad (8)$$

$$L^2\nabla^2 f - f = \frac{1}{\tau}\left(c_1 + C_2'\frac{\mathscr{P}}{\varepsilon}\right)\left(\zeta - \frac{2}{3}\right) \quad (9)$$

[1] In the course of the manuscript review it was brought to our attention that Laurence et al. (2004) have been pursuing a similar idea.

$$\frac{D\zeta}{Dt} = f - \frac{\zeta}{k}\mathscr{P} + \frac{\partial}{\partial x_k}\left[\left(\nu + \frac{\nu_t}{\sigma_\zeta}\right)\frac{\partial \zeta}{\partial x_k}\right] \tag{10}$$

The model is completed by imposing the Kolmogorov time and length scale as the lower bounds, combined with Durbin's (1996) realizability constraints:

$$\tau = \max\left[\min\left(\frac{k}{\varepsilon}, \frac{a}{\sqrt{6}C_\mu \mid S \mid \zeta}\right), C_\tau\left(\frac{\nu}{\varepsilon}\right)^{1/2}\right] \tag{11}$$

$$L = C_L \max\left[\min\left(\frac{k^{3/2}}{\varepsilon}, \frac{k^{1/2}}{\sqrt{6}C_\mu \mid S \mid \zeta}\right), C_\eta\left(\frac{\nu^3}{\varepsilon}\right)^{1/4}\right] \tag{12}$$

where $a \leq 1$ (recommended $a = 0.6$). The following coefficient are recommended (note the reformulation of $C_{\varepsilon 1}$):

to the first y^+ used for DNS. The computation convergence rate shown in Fig. 2 shows that the computation with ζ–f is much more stable and robust than with the $\overline{v^2}$–f model.

Fig. 3 presents the mean velocity profiles, and Fig. 4 shows Stanton number along the bottom wall behind a step in a backward facing step flow. Velocity profiles obtained with the two models at several locations within the separation bubble and around reattachment are practically indistinguishable and both in good agreement with experiments of Vogel and Eaton (1985). A small difference appears in the Stanton number, but in view of experimental uncertainty, the results can be considered as fully satisfactory.

Figs. 5 and 6 give respectively the mean velocity profiles and Nusselt number in a round jet issuing from a fully developed pipe flow and impinging normally on a plate. The distance between the pipe exit and the plate is $H/D = 2$. The results are compared with experiments of Baughn and Shimizu (1989) and Baughn et al. (1991) for the Nusselt number and Cooper et al. (1993) for the velocity field, as well as the $\overline{v^2}$–f computations using the coefficients of Behnia et al. (1998). The velocity profiles are similar with some improvements returned by the ζ–f model, especially for $r/D = 3.0$. Similar quality of predictions has been obtained for the Nusselt number where ζ–f model shows some slight overprediction, but a more realistic shape of the curve.

C_μ	$C_{\varepsilon 1}$	$C_{\varepsilon 2}$	c_1	C_2'	σ_k	σ_ε	σ_ζ	C_τ	C_L	C_η
0.22	1.4(1 + 0.012/ζ)	1.9	0.4	0.65	1	1.3	1.2	6.0	0.36	85

4. The ζ–f model with $f_w = 0$

One can make further simplifications to satisfy zero wall boundary condition for f_w (in analogy with the original Jones and Launder (1972) formulation of the low-Re-number dissipation equation) by solving Eq. (9) but for $\tilde{f}$ with $\tilde{f}_w = 0$ and getting f from:

$$f = \tilde{f} - 2\nu\left(\frac{\partial \zeta^{1/2}}{\partial x_n}\right)^2 \tag{13}$$

which is then used in ζ equation. The second term on the right of Eq. (13) is just an alternative for $2\nu\zeta/y^2$, which follows closer the polynomial expansion of ζ around $y = 0$.

5. Some illustrations

As an illustration of performance of the ζ–f model, we present some results of computation of velocity fields and heat transfer in three common test cases: a plane channel flow, a separating flow behind a backward facing step and in a round impinging jet. The temperature field was obtained by solving the RANS energy equation with constant fluid properties, using the isotropic eddy diffusivity ν_t/σ_T where ν_t is given by Eq. (6) and $\sigma_T = 0.9$.

In Fig. 1 profiles of velocity and turbulent quantities are shown for a channel flow at $Re_\tau = 590$, and compared with the DNS of Moser et al. (1999). Note that results with ζ–f model are obtained with the mesh with the wall-nearest cell-center at $y^+ = 0.01$, which corresponds

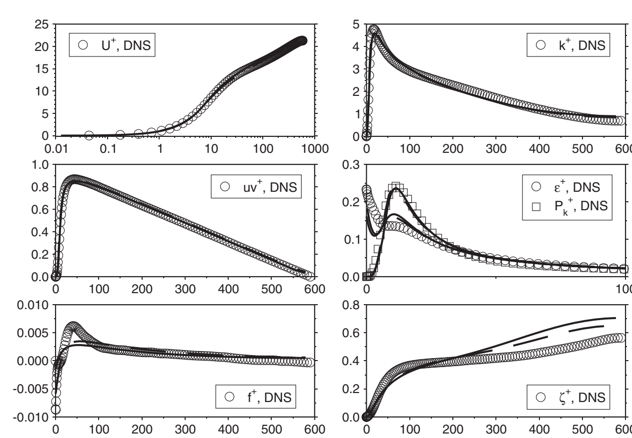

Fig. 1. Velocity and turbulent quantities in channel flow $Re_\tau = 590$. Symbols: DNS data of Moser et al. (1999). Full line: ζ–f; dotted line: $\overline{v^2}$–f model.

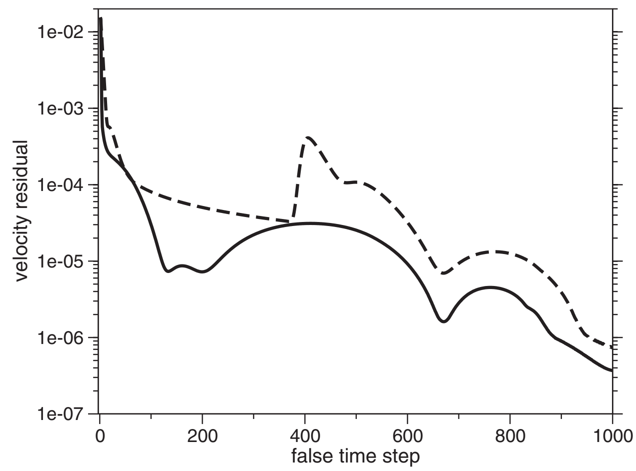

Fig. 2. Channel flow, $Re_\tau = 590$, Convergence histogram. Full line: ζ–f; dotted line: $\overline{v^2}$–f model.

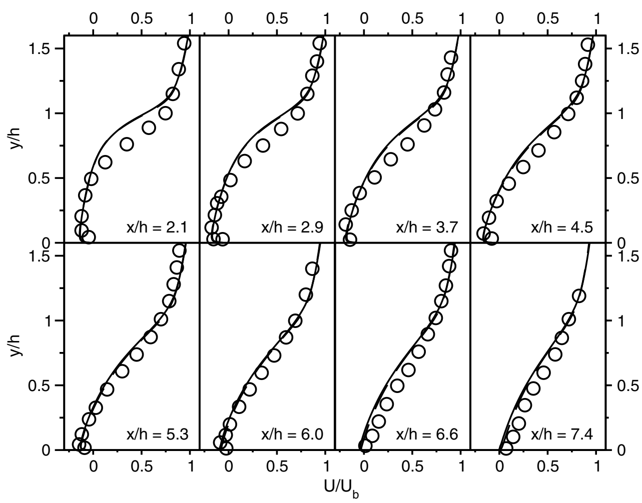

Fig. 3. Velocity profiles in a backward-facing step flow ($Re = 28000$). Symbols: experiments of Vogel and Eaton (1985). Full line: ζ–f; dotted line: $\overline{v^2}$–f model.

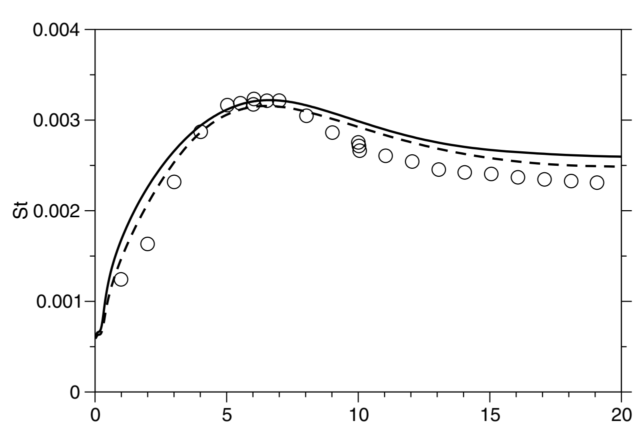

Fig. 4. Stanton number in a backward-facing step ($Re = 28000$). Symbols: experiments of Vogel and Eaton (1985). Full line: ζ–f; dotted line: $\overline{v^2}$–f model.

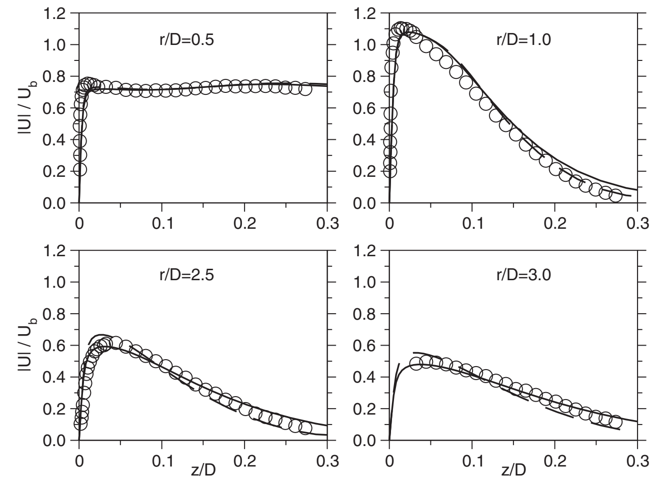

Fig. 5. Impinging jet ($Re = 23000$): velocity profiles at different distances from the jet center. Symbols: experiments of Cooper et al. (1993). Full line: ζ–f; dotted line: $\overline{v^2}$–f model.

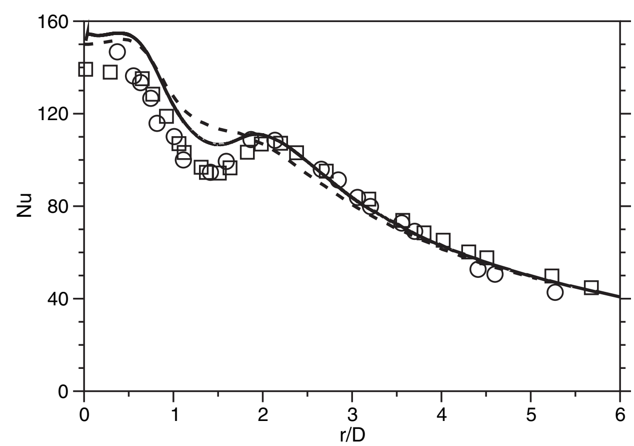

Fig. 6. Impinging jet ($Re = 23000$): Nusselt number, Symbols: experiments of Baughn and Shimizu (1989) and Baughn et al. (1991). Full line: ζ–f; dotted line: $\overline{v^2}$–f model.

Acknowledgments

This work emerged from the MinNOx project sponsored by the Commission of the European Community, Contract ENK6-CT-2001-00530.

References

Baughn, J., Shimizu, S., 1989. Heat transfer measurements from a surface with uniform heat flux and an impinging jet. ASME J. Heat Transfer 111, 1096–1098.

Baughn, J.W., Hechanova, A.E., Yan, X., 1991. An experimental study of entrainment effects on the heat transfer from a flat surface to a heated circular impinging jet. J. Heat Transfer 113, 1023–1025.

Behnia, M., Parniex, S., Durbin, P.A., 1998. Prediction of heat transfer in an axisymmetric turbulent jet impinging on a flat plate. Int. J. Heat Mass Transfer 41, 1845–1855.

Cooper, D., Jackson, D.C., Launder, B.E., Liao, G.X., 1993. Impinging jet studies for turbulence model assessment –Part 1. Flow-field experiments. Int. J. Heat Mass Transfer 36, 2675–2684.

Durbin, P.A., 1991. Near-wall turbulence closure modelling without damping functions. Theor. Comput. Fluid Dyn. 3, 1–13.

Durbin, P.A., 1996. On the k–ε stagnation point anomaly. Int. J. Heat Fluid Flow 17, 89–90.

Jones, W.P., Launder, B.E., 1972. The prediction of laminarization with a two-equation model of turbulence. Int. J. Heat Mass Transfer 15, 301–314.

Laurence, D.R., Uribe, J.C., Utyuzhnikov, S.V., 2004. A robust formulation of the v2–f model. Flow, Turbulence and Combustion, in press.

Lien, F.S., Kalitzin, G., Durbin, P.A., 1998. RANS modeling for compressible and transitional flows. Proc. Summer Program, 267–286.

Moser, R.D., Kim, J., Mansour, N.N., 1999. Direct numerical simulation of turbulent channel flow up to $Re_\tau = 590$. Phys. Fluids 11, 943–945.

Speziale, C.G., Sarkar, S., Gatski, T., 1991. Modelling the pressure–strain correlation of turbulence: an invariant system dynamic approach. J. Fluid. Mech. 227, 245–272.

Vogel, J.C., Eaton, J.K., 1985. Combined heat transfer and fluid dynamic measurements downstream of a backward-facing step. ASME J. Heat Transfer 107, 922–929.